applied sciences

MDPI

Article

Effect of Different Gradings of Lightweight Aggregates on the Properties of Concrete

Sang-Yeop Chung [1], Mohamed Abd Elrahman [1,2,*] and Dietmar Stephan [1]

[1] Building Materials and Construction Chemistry, Technische Universität Berlin, Gustav-Meyer-Allee 25, 13355 Berlin, Germany; sychung419@gmail.com (S.-Y.C.); stephan@tu-berlin.de (D.S.)

[2] Structural Engineering Department, Mansoura University, Elgomhouria St., Mansoura City 35516, Egypt

* Correspondence: mohattia76@gmail.com; Tel.: +49-030-314-72-104

Academic Editor: Peter Van Puyvelde

Received: 20 April 2017; Accepted: 1 June 2017; Published: 7 June 2017

Abstract: Lightweight aggregate concrete is a material with very low density and good thermal insulation, and several types of lightweight aggregates have been used for lightweight concrete. Since the characteristics of lightweight aggregates strongly affect the properties of lightweight concrete, a proper consideration for the use of lightweight aggregate is very important for development of lightweight materials. In particular, the sizes and spatial distributions of lightweight aggregates can influence the material responses of lightweight concrete, such as compressive strength and thermal conductivity. In this study, different types of gradings of lightweight aggregates are adopted to investigate the effect of gradings on the material properties. Liaver®, an expanded glass granulate, is used as a lightweight aggregate for the specimens. Virtual models of the lightweight specimens with different gradings are numerically generated, and both mechanical and thermal properties are evaluated using experimental and numerical approaches for more detailed investigation. The obtained results can be utilized to suggest an optimal grading that satisfies both the mechanical and thermal properties of lightweight concrete specimen.

Keywords: lightweight aggregate concrete; grading; material design; thermal conductivity; compressive strength

1. Introduction

Concrete is a representative building material and has a very important role in the construction field. Since the control of energy consumption has become a worldwide issue, many efforts have been performed to enhance energy efficiency in the field of building and concrete materials. Among the various types of concrete for special applications, lightweight concrete has been widely used due to its advantageous characteristics, such as lower density and higher insulation effect than those of conventional concrete [1,2]. According to EN 206, lightweight concrete is a material with density lower than 2000 kg/m^3, and it contains natural or synthetic lightweight aggregates (lightweight aggregate concrete) or foam agent (foamed concrete) to reduce the weight of material; this material can be used for both structural and nonstructural purposes, i.e., insulation and concrete block [3,4].

To produce lightweight aggregate concrete, several types of materials have been used as lightweight aggregates. Sales et al. [5] used sawdust and water treated sludge as lightweight aggregates and confirmed its effect to reduce the environmental impact. Chabannes et al. [6] utilized raw rice hush for lightweight concrete and demonstrated that the material can be used as a filling material to improve the mechanical performance of concrete. Wu et al. [7] used hollow cenospheres from fly ash as lightweight aggregates for the material and confirmed its effect on the improvement of tensile strength. Colangelo et al. [8] used a recycled municipal solid waste incinerator (MSWI) fly ash as lightweight aggregates and showed that the material can effectively be utilized as lightweight

aggregates with average performance. Lihua et al. [9] used ferrochromium slag to improve the performance of lightweight concrete and confirmed that the material endowed a dense microstructure and high bond strength of the interfacial transition zone. Bogas and Cunha [10] produced lightweight concrete with volcanic scoria aggregates, and the obtained material showed better mechanical behavior at high temperatures than conventional concrete. Colangelo et al. [11] used recycled polyolefins waste and demonstrated that this material can be used as a sustainable practice in lightweight concrete manufacturing. Guneyisi et al. [12] utilized nanosilica for lightweight concrete and showed its impact on the workability of self-compacting lightweight concrete. Youm et al. [13] evaluated the performance of the material with silica fume for 91 days and confirmed its advanced durability against chemical deterioration. In addition, artificial lightweight aggregates, such as Poraver® (Postbauer-Heng, Germany), Leca® (Randers SV, Denmark), and Liaver® (Ilmenau, Germany), are also utilized for lightweight aggregate concrete due to their low densities and advanced properties [14].

In general, lightweight aggregates occupy more than 50% of the volume of concrete, and the total volume of the lightweight aggregates is a significant factor to determine the properties of lightweight concrete. For example, the density of lightweight concrete, which is a factor that strongly affects both mechanical and thermal properties, varies between 800 and 1500 kg/m^3 depending on the volume of lightweight aggregates [15], and when the specimen contains a large volume of lightweight aggregates, the density and thermal conductivity decrease, while the stiffness and compressive strength also tend to decrease [16]. In addition, the physical properties of lightweight concrete, such as density, and mechanical and thermal properties, are affected significantly by the characteristics of lightweight aggregates [17]. Therefore, a proper use of the lightweight aggregates should be carefully considered to produce lightweight concrete with acceptable performance for both mechanical and thermal responses. Among several characteristics of aggregates, the grading (or particle size distribution) of lightweight aggregates is a very important factor because it can affect the workability and cost of concrete [18]. In particular, it is desirable for lightweight concrete to contain large volume of lightweight aggregates to reduce the density and to minimize the use of cement. For this purpose, the use of appropriate grading of aggregates is required to include large volume of lightweight aggregates in the specimen.

The main objectives of this study can be summarized as follows: (1) production of lightweight aggregate concrete (LWC) with very low density (less than 500 kg/m^3) by maximizing lightweight aggregate volume using different gradings of lightweight aggregates (LWA); (2) evaluation of the material responses using experimental and numerical approaches; and (3) investigation of the effect of different gradings on the material characteristics and properties. Here, Liaver® (Ilmenau, Germany), an expanded glass granulate, is used as lightweight aggregates for lightweight concrete specimens according to its very low density and water absorption characteristics; this material is produced by being ground, granulated, distended and vitrified in a rotary kiln at 750 °C to 900 °C, and this produces very light granules measuring between 100 µm and 16 mm grain diameter. [19]. Different gradings following the modified Andreasen and Andersen dense packing model [20–23] are adopted to produce the lightweight specimens with densely packed Liaver® particles. Here, the target volume of lightweight aggregates is more than 70% of the concrete volume. To investigate the effect of the gradings on the material properties, elastic modulus, compressive strength, and thermal conductivity values of lightweight concrete specimens are evaluated using experimental and numerical approaches; experimental tools, such as testing compressive strength (Toni Technik, Berlin, Germany) and thermal conductivity by the transient plane source method (Hot Disk, Göteborg, Sweden), are adopted to measure the mechanical and thermal properties, respectively. For the numerical lightweight specimens, random packing models of particles with different size distributions are adopted here [24–26], and their responses are computed using finite element (FE) analysis. In addition, X-ray computed tomography (CT) is utilized to investigate the inner structures of the lightweight concrete specimen without destruction of the samples; the aggregate structures are investigated by incorporating a probabilistic description method, the lineal-path function, to describe the size characteristics of the lightweight

aggregates within the specimens. Then, the correlation of the gradings and the material properties is discussed.

2. Experimental Investigation

2.1. Constituent Materials

In this study, four different mixes with different gradings have been designed and manufactured. To produce the specimens, CEM III A 42.5 N provided by HeidelbergerCement (Heidelberg, Germany) is used, and condensed silica fume (SF) is also used for the replacement of 10% cement by weight to enhance the mechanical properties of lightweight concrete. Detailed information about the chemical composition and physical properties of both cement and silica fume are listed in Table 1. Expanded glass type aggregate (Liaver®), provided by Liaver Company (Ilmenau, Germany) in Figure 1, is used with various fractions. Physical properties of the expanded glass aggregate can be found in Table 2. An ether-based polycarboxylic (Sika Viscocrete 1051, Hamburg, Germany) with a density of 1.04 g/cm^3 is used to achieve consistency class F3/F4 according to EN 206-1. To prevent segregation and improve the stability of the mix, a viscosity modifying admixture (Sika stabilizer, type 10160317) is used.

Table 1. Chemical and physical properties of cement and silica fume [wt %].

Material	CaO	SiO_2	Al_2O_3	Fe_2O_3	MgO	Na_2O	K_2O	SO_3	Cl	Specific Density	Surface Area (cm^2/g)
Cement [wt %]	54.8	23.7	8.8	1.46	5.21	0.3	0.59	2.4	-	3.05	3860
Silica fume [wt %]	0.2	98.4	0.2	0.01	0.1	0.15	0.2	0.1	0.01	2.2	200,000

Figure 1. Expanded glass aggregate (Liaver®) and its microscopy images.

Table 2. Physical properties of the lightweight aggregates (LWA).

Material	Bulk Density (kg/m^3)	Specific Density	Crushing Resistance * (MPa)	Water Absorption ** [wt %]	
				60 min	24 h
Liaver® 0.5–1.0	250	450	2.6	12.08	21.8
Liaver® 1.0–2.0	220	330	2.4	13.96	26.5
Liaver® 2.0–4.0	190	310	2.2	11.5	27.1

* according to EN 13055-1; ** according to EN 1097-6.

2.2. Mix Design Methodology

An optimization of a lightweight concrete (LWC) mixture is not so simple because this type of concrete is very sensitive to any change in its components that affect its stability and properties significantly. One important target of this study is to minimize the density of the material. For this purpose, increasing the lightweight aggregate content, which is the lightest component in the concrete mixture, is a good option to reduce the material density; this can be achieved by applying a dense

packing concept without a negative effect on the material properties. The idea of this concept is that if a large volume of aggregate can be efficiently packed in a certain volume, then the gaps between the aggregates can be minimized, and thereby the required paste to fill the gaps is considerably decreased [27]. In this study, LWC mixture proportions are selected based on the granular optimization of solid materials by means of the Andreasen and Andersen model [20] as:

$$P(D) = \frac{D^q - D_{min}^q}{D_{max}^q - D_{min}^q}, \quad (1)$$

where $P(D)$ is the total fraction passing through a sieve with the particle size D. D_{max} is the maximum particle size, D_{min} is the minimum particle size, and q is the distribution factor [17,28]. There are several suggestions on the selection of the q value. Some researchers found that q = 0.37 gives the optimal packing [23,29], while others suggested that q = 0.28 is the ideal case [30,31]. The factor q can be experimentally determined, and it depends upon the size and shape of the particles. Higher values of q lead to coarse mixtures with lower fine content; however, lower values lead to mixtures with higher fine materials content. Yu et al. [32] used q = 0.37 to develop ultra-lightweight concrete and claimed that this value can give the optimal packing for self-compacting concrete. In this study, four different values of q (0.23, 0.25, 0.30, and 0.45) are used to investigate the effect of the grading on the material properties, and the specimens with different q-values are denoted here as LW 23, LW 25, LW 30 and LW 45, respectively. The proportions of different aggregate sizes are presented in Figure 2 and Table 3. All mixes have the same cementitious material compositions, and the mix proportions of the specimens are presented in Table 4.

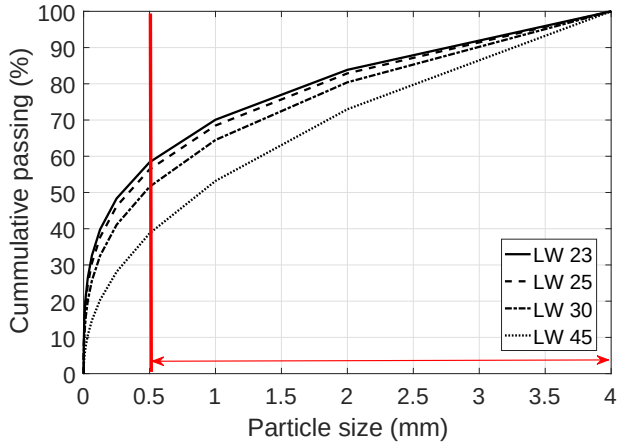

Figure 2. Gradings of different mixes (note: in this study, particles larger than 0.5 mm diameter are used for the specimens.).

Table 3. Volume proportions of lightweight aggregates (Liaver®) in each sample.

Sample	q	Proportion of Liaver® Volume		
		Liaver® 0.5–1.0 mm	Liaver® 1.0–2.0 mm	Liaver® 2.0–4.0 mm
LW 23	0.23	0.2818	0.3305	0.3877
LW 25	0.25	0.2565	0.3269	0.4165
LW 30	0.30	0.4210	0.2664	0.3126
LW 45	0.45	0.3489	0.2751	0.3760

Table 4. Mix proportions of concrete mixes.

Sample	Cement (kg/m^3)	Silica Fume (kg/m^3)	SP* (kg/m^3)	ST** (kg/m^3)	Water (kg/m^3)	LWA (kg/m^3)		
						2.0–4.0 mm	1.0–2.0 mm	0.5–1.0 mm
LW 23	216	24	4.32	0.72	182.4	75.4	80.7	74.36
LW 25	216	24	4.32	0.72	182.4	67.04	80.8	75.48
LW 30	216	24	4.32	0.72	182.4	80.1	80	68.7
LW 45	216	24	4.32	0.72	182.4	82.4	79.46	65.9

* SP: superplasticizer; ** ST: stabilizer.

Contrary to normal aggregates, the water absorption of LWA is a considerable factor that affects the workability of LWC significantly. It has a negative effect on the concrete workability, especially with transport concrete, which should be workable for a long time. For this reason, the water absorptions of LWC have been measured according to EN 1097-6 at 60 min and 24 h. In general, two mixing procedures are developed for LWC: pre-soaking the aggregates for 24 h and adding an extra amount of water, which equals the 1 h water absorption of LWC. In this study, a certain amount of water that equals the water absorption of aggregate in 60 min is added to the mixing water in order to keep the concrete workability for a long time. The fresh properties of the specimens are presented in Table 5.

Table 5. Fresh properties of the samples.

Sample	Density of Fresh Concrete * (kg/m^3)	Flow Diameter ** (mm)
LW 23	644–655	512
LW 25	642–646	520
LW 30	654–670	495
LW 45	640–660	508

* according to EN 12350-6; ** according to EN 12350-5.

2.3. Preparation of Samples and Test Methods

A concrete mixer with a capacity of about 60 L is used to mix the concrete. The mixing procedures for all mixes are performed in the same condition. After mixing, the molds are casted without compaction and kept in a controlled conditions of temperature of 21 ± 1 °C. After 24 h, the test specimens were removed from the molds, and the curing process performed under water until the day of testing. Several tests have been carried out at the age of 28 days including the compressive strength test on cubes with size 100 × 100 × 100 mm^3 according to EN 12390-3. The elasticity of concrete is measured using cylinders (150 × 300 mm) according to EN 1048-5. The dry density of concrete is also determined after totally drying the samples at 105 °C until a constant mass. The thermal conductivity is measured using the transient plane source method (Hot Disk, Göteborg, Sweden) that meets the ISO standard 22007-2 [33], and the compressive strength is also measured using the testing machine (Toni Technik, Berlin, Germany) that satisfies the EN 12390-4 [34]. All tests have been carried out on three specimens and the mean value is considered in each case.

3. Numerical Modeling and Characterization

To investigate the material properties of the lightweight concrete specimens in numerical manner, the samples with different aggregate compositions in Figure 1 are modeled, and their properties, such as the compressive strength and thermal conductivity, are computed using FE analysis. The grading characteristics of the lightweight aggregates are described using the probabilistic method. X-ray CT images are also utilized to examine the characteristics of the lightweight aggregates within the real specimens.

3.1. Numerical Modeling with a Dense Packing Algorithm

3.1.1. Virtual Specimens with Different Gradings

The same gradings in Section 2.1 are adopted for virtual (numerical) lightweight concrete specimens. Several random packing algorithms are proposed by different researchers [24,25,35]. In this study, a packing theory used by Sobolev and Amirjanov [26] is utilized to generate the virtual specimens. In their model, particle packings with three different size distributions, such as mono size, bimodal, and Gaussian, can be produced; here, the modified bimodal distribution model is adopted, and a detailed description of the model can be found in [26,36].

To produce the virtual specimens with different gradings, the LWA is classified into four classes as 4, 2, 1, and 0.5 mm particle sizes, and ±5% differences in each class are set to be allowed. In each virtual specimen, every Liaver® particle is assumed to be non-overlapping spheres and are randomly distributed by considering the packing algorithm and interparticle reactions. Figure 3 shows the sample of the virtual LWC specimens with different gradings. In each sample, the ratios between different sizes of LWA are assumed to be the same as those of the real LWC specimens in Section 2.3, and designed volume content of LWA in each specimen is about 73% of the whole specimen. The remaining part is considered as the matrix (cement paste). The material properties of LWAs with different sizes and matrices are presented in Table 6. The characteristics of the LWA size distribution and material responses are evaluated using these samples as well as numerical approaches and compared with those from experimental results.

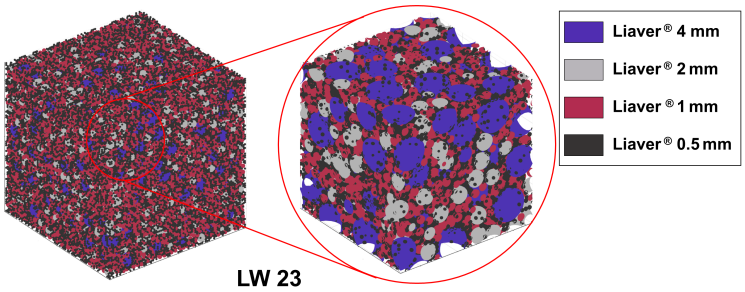

Figure 3. Sample of virtual specimens with different gradings (note: each color denotes spherical Liaver® with different sizes. The total volume of Liaver® particles in each specimen is about 73%.).

Table 6. Material properties of lightweight aggregates (Liaver®) and matrix [19].

Types	Matrix (Mortar)	Liaver® 4 mm	Liaver® 2 mm	Liaver® 1 mm	Liaver® 0.5 mm
Thermal Conductivity (W/m/K)	0.31	0.070	0.073	0.075	0.080
Density (kg/m^3)	1047	310	340	350	450
Specific Heat (J/kg/K)	960	1200	1150	1140	1100
Elastic Modulus (GPa)	8.15	0.76	0.79	0.80	0.84
Poisson's Ratio	0.3	0.37	0.37	0.36	0.36
Yield Strength (MPa)	40.78	1.2	2.2	2.4	2.9

3.1.2. Numerical Simulations

The material properties of the virtual specimens, the elastic modulus, compressive strength, and thermal conductivity are numerically computed using the FE simulation. For the calculation, ABAQUS commercial software [37] (v2016, Dassault Systemes, Velizy-Villacoublay Cedex, France) is used. In particular, a concrete damaged plasticity (CDP) model in the ABAQUS package is used here to examine the mechanical responses. Detailed formulations for mechanical and thermal analysis can be found in [38,39] (mechanical) and [40,41] (thermal), and only general formulations are given in this paper.

For the mechanical analysis, the governing equation for the stress–strain relationship controlled by a scalar damaged elasticity is described as:

$$\boldsymbol{\sigma} = (1-d)\boldsymbol{D}_0^{el} : (\boldsymbol{\epsilon} - \boldsymbol{\epsilon}^{pl}) = \boldsymbol{D}_0 : (\boldsymbol{\epsilon} - \boldsymbol{\epsilon}^{pl}), \tag{2}$$

where $\boldsymbol{\sigma}$ is the stress tensor, and d is the scalar stiffness degradation variable that can take values from 0 (undamaged state) to 1 (fully damaged state). $\boldsymbol{D}_0^{el}$, $\boldsymbol{D}_0$, $\boldsymbol{\epsilon}$, and $\boldsymbol{\epsilon}^{pl}$ are the initial elastic modulus, the degraded elastic stiffness, the total strain tensor, and the plastic strain tensor, respectively.

For the boundary conditions, a displacement boundary condition is imposed on the top surface of the samples, and the opposite surface is set to be a fixed boundary condition. The required input parameters for the simulation, such as elastic modulus, yield compressive strength, and diliation angle, are selected from the analytical formulations in [38,39,42].

To investigate heat transfer characteristics of the specimens, the required governing equation with considering the heat loss parameter can be modified and described as:

$$\frac{\partial T}{\partial t} = \frac{k}{\rho C}\left(\frac{\partial^2 T}{\partial x^2} + \frac{\partial^2 T}{\partial y^2} + \frac{\partial^2 T}{\partial z^2}\right) - \lambda \cdot T^*, \tag{3}$$

where T [K], T^* [K], and t [s] are the temperature, the surrounding temperature, and the time, respectively. k [W/m/K] is the thermal conductivity, ρ [kg/m^3] is the mass density, C [J/g/K] is the specific heat, and λ [1/s] is the heat loss coefficient. Equation (3) is integrated for the weak form of the governing equation. Then, the effective heat flux and the effective thermal conductivity can be calculated using Fourier law [40,41].

The input parameters, such as material thermal conductivity, density, and specific heat, are measured using the Hot Disk device [33]. Boundary conditions for the simulation are imposed on the top and bottom surfaces of the specimens as: a constant temperature (60 °C) on the top surface, heat loss on the opposite surface with the heat loss coefficient of 1.3 [1/s], and the surrounding temperature of 23 °C. Other remaining surfaces are assumed to have no heat loss.

3.2. Probabilistic Characterization Method and CT Measurement

3.2.1. Lineal-Path Function

The main objective of this study is to investigate the correlation between the size characteristics and the properties of the LWC specimens with different gradings. Therefore, to characterize the LWA size distribution, a proper description method is needed. The lineal-path function, a type of low-order probabilistic function, can be used to describe the continuous connectivity of a specific component, such as aggregate and pore [43–45]; this function can be utilized to characterize the aggregate size distribution. The lineal-path function, $L_{lwa}(r)$, is the probability that a randomly distributed line segment with length r is located in the LWA phase, which is denoted as lwa. $L_{lwa}(r)$ approaches the volume ratio of the lightweight aggregates as the line length becomes zero, while the probability of the whole line segment is in the lightweight aggregate approaches zero with the line length going to infinity as:

$$\lim_{r\to 0} L_{lwa}(r) = f_{lwa}, \qquad \lim_{r\to\infty} L_{lwa}(r) = 0, \tag{4}$$

where f_{lwa} is the LWA volume ratio in the specimen. Here, this function is adopted to describe the relative LWA sizes in the specimens.

3.2.2. X-ray CT Measurement

Several approaches, such as scanning electron microscopy (SEM) and optical microscope (OM), can be used to identify the material characteristics. Although they have many advantages, these methods have critical limits to investigate the material characteristics and the inner structures without damaging

the samples. To overcome the limitations, X-ray micro-computed tomography (CT), a non-destructive method, is used here to investigate the inner structures of the LWC specimens. Using CT images, the spatial and size distributions of LWAs within the specimens can be investigated without destructing the samples.

In this study, an X-ray radioscopy measurement tool developed to observe the material structure is utilized [46]. For more effective investigation of the LWA distribution in the specimen, an imaging processing for converting the original 8-bit (grayscale) to a binary (black and white) image is conducted, as shown in Figure 4. For the imaging, the image processing toolbox in MATLAB (R2016a) is used here. In this figure, Figure 4a is the original 8-bit CT image of the region of interest (ROI). The image in Figure 4a is composed of 1400 × 1400 pixels with 27.5 μm pixel size, which is sufficient to describe the LWAs. Each pixel in the 8-bit grayscale image is represented by a value between 0 and 255, where 0 is black and 255 is white. For the binarization, a proper threshold value should be selected to classify aggregate and matrix from the original CT image, and the threshold is chosen by using the Otsu method [47] as well as mix design. Here, a set of pixels smaller than the threshold value is considered as an aggregate with the white, while the black represents the matrix part of the specimen including pores, as shown in the binary image in Figure 4b. To classify each aggregate, the watershed segmentation algorithm [48] is adopted here as shown in Figure 4c. Then, the 3D image in Figure 4d is generated by stacking a series of binary images, and the characteristics of the LWAs in the specimens are examined numerically using the obtained 3D images.

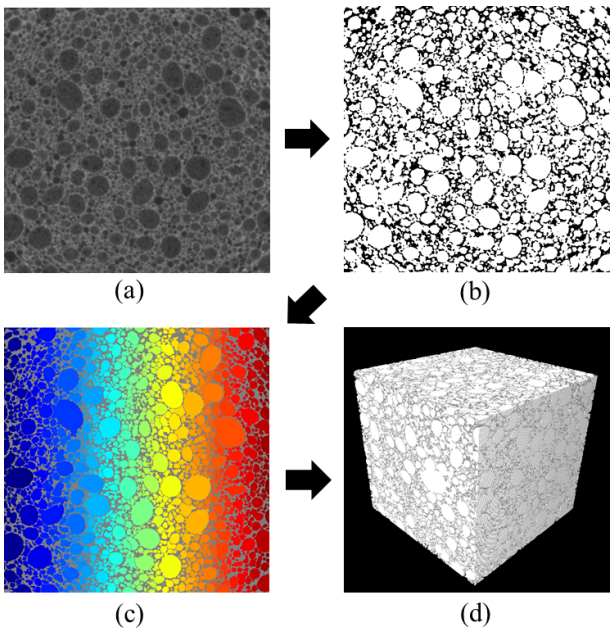

Figure 4. CT imaging of LWC specimen (LW 23): (**a**) region of interest (ROI) of the original 8-bit CT image; (**b**) binarized image; (**c**) classification of lightweight aggregates; (**d**) 3D image of lightweight aggregate part (note: in the binary image (**b**), the white represents aggregate parts, and the black represents mortar parts of the specimen. In the Figure (**c**), each color denotes a distinct aggregate.).

4. Evaluation of the Properties of Concretes with Different Aggregate Gradings

The material properties, such as elastic modulus, compressive strength, and thermal conductivity, are evaluated using both experimental and numerical methods. In addition, the characteristics of the aggregate size distributions are described using the probability function. The inner structures of the lightweight aggregate concrete specimens are also investigated using X-ray CT imaging, and the effects of gradings on the material characteristics are discussed.

4.1. Mechanical Property Evaluation

The mechanical properties, elastic modulus and compressive strength, are evaluated. For the experiments, the mechanical loading tools that satisfy the German (elastic modulus) and European (compressive strength) standards are used. The numerical properties are also computed using the ABAQUS package and compared with those from the experiments.

Figure 5 shows the results of elastic modulus and compressive strength of the LWC specimens obtained from the experiments and simulations. As can be seen in these figures, all the LWC samples produced here have the density less than 500 kg/m^3, which is consistent with the objective of this study. In Figures 5a,b, general trends of the mechanical properties are almost the same, although the differences in the elastic modulus are relatively larger than that of the compressive strength; the elastic modulus and the compressive strength of LW 30 are the largest among all cases, while those of LW 23 is the smallest. In addition, both properties tend to increase as the density of the specimen increases, except the case of LW 23. The differences between the experiments and simulations are mainly due to the assumption of the numerical model; all the aggregates in the virtual samples are set to be perfect spheres, and this will be discussed in detail in Section 4.3. Among the samples, LW 30 includes the largest proportion of fine aggregates (Liaver® 0.5–1.0 mm) and the smallest volume of coarse aggregates (Liaver® 2.0–4.0 mm). Comparing the mechanical properties of LW 23 and LW 45, which have similar experimental densities, the elastic modulus and the compressive strength are larger when the proportion of fine aggregates is larger; this denotes that the lightweight concrete can have improved mechanical properties by controlling the size distribution of LWAs.

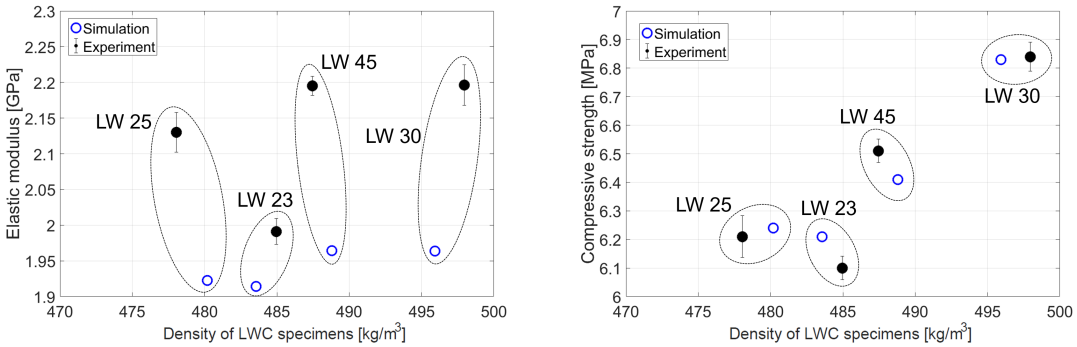

Figure 5. Comparison of mechanical properties of the LWC samples: (**a**) elastic modulus; (**b**) compressive strength.

In general, it is well known that the compressive strength value is the main factor to evaluate the efficiency of normal weight concrete. However, in the case of LWC, not only compressive strength, but also a thermal insulation property should be considered for the concrete development. Thermal properties of cementitious materials are mainly controlled by the pore size distributions as well as the total pore volume, or in other words, by the dry density; therefore, in order to evaluate the performance of lightweight concrete, both density and compressive strength should be carefully considered. In this study, the following formula is used to calculate the efficiency factor [49]:

$$F_{eff} = [F_c/(p/2.2)]^{2.5}, \quad (5)$$

where F_{eff} is the efficiency factor, F_c is the compressive strength at 28 days [N/mm^2], and p is the dry density of concrete in [t/m^3]. It has been suggested that high performance LWC shows an efficiency factor higher than 70 [49]. By applying the formula, all four of the mixes have efficiency factors of 275–280, which are much higher than that of conventional high performance LWC. This can be explained by the high content of LWA due to applying the packing density concept. By increasing the

LWA content, which is much lighter than cement and water, ultra LWC can be produced. In addition, by enhancing the packing of particles, the pores between the particles are minimized, and the required cement paste to fill these pores are also minimized.

The results in Figure 5 demonstrate that all the samples, which are designed by considering the packing algorithm, have higher mechanical performances with lower densities than those of conventional LWC. In particular, the LWC specimen with a larger proportion of finer aggregates in the same volume of aggregates shows a higher elastic modulus as well as compressive strength, although the density of the specimen becomes larger when the proportion of finer aggregates increases.

4.2. Thermal Property Evaluation

The thermal responses of the LWC samples are experimentally and numerically investigated. The Hot Disk device that satisfies the European standard is used to measure the thermal conductivities of the LWC samples, and three to five specimens in each case are repeatedly measured on different sides of the specimens to increase accuracy. The obtained thermal properties from the experiments are utilized for the numerical simulation and compared with those data. Here, the ABAQUS package is also used for the simulation, and the sample investigation is presented in Figure 6.

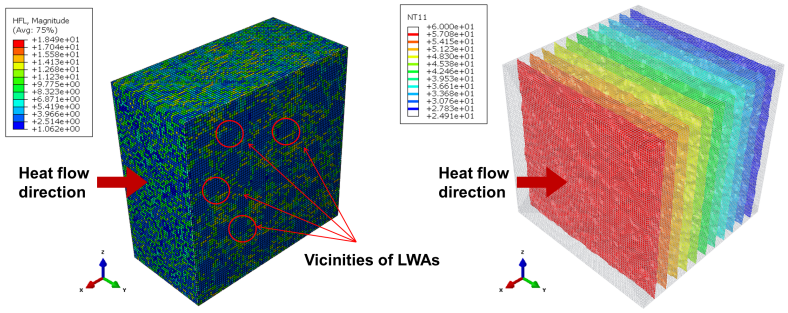

Figure 6. The sample view cut of heat flux contour (**left**) and temperature distribution (**right**) for LW 23.

Figure 7 presents thermal conductivity values of the samples obtained from both experimental and numerical methods with respect to the specimen density. In this figure, a general trend of the thermal conductivity related to the density and grading can be identified. Likewise, for the mechanical cases in Figure 5, LW 30 shows the largest thermal conductivity as well as the specimen density, while LW 25 has the lowest values; this denotes that the thermal conductivity of LWC is also affected by the density of the specimen. In addition, the thermal conductivity values of LW 23 and LW 45 show differences for both experiments and simulations, even though their experimental densities are almost the same. However, LW 23 and LW 25 have different experimental densities, although their thermal conductivity values are almost the same in both experimental and numerical approaches. This indicates that the thermal conductivity of LWC can be affected by the density as well as the type of grading of LWA; when the specimen density is almost the same, the specimen that contains less volume of finer aggregates shows lower thermal conductivity (LW 23 and LW 45), while the specimens with different densities can have almost the same thermal property by adopting an appropriate grading (LW 23 and LW 25).

4.3. Verification of Specimens with X-ray CT and the Probabilistic Method

The effect of grading on the characteristics of the LWC specimens is investigated using X-ray CT and the lineal-path function. Figure 8 presents the 3D LWA images of each LWC specimen, and the differences between the specimens are visualized in these figures. For example, it can be roughly identified that LW 25 contains coarser LWAs than other samples. The shapes and the structures of

LWAs in each specimen can also be examined. The 2D and 3D images in Figure 8 demonstrate that LWAs in the specimens are densely packed and their shapes are not perfect spheres, although the aggregates are tended to be round shaped; this causes the difference between the experimental and numerical properties for both mechanical and thermal responses in Figures 5 and 7.

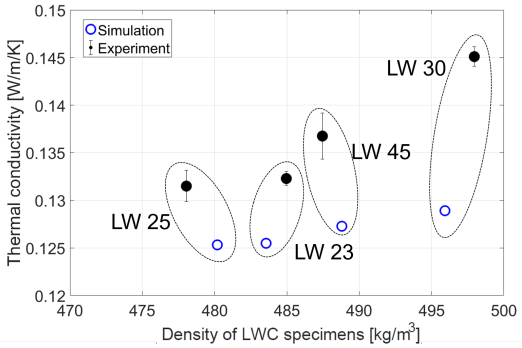

Figure 7. Comparison of thermal conductivities of the LWC samples.

The qualitative comparison of the LWA distributions in each specimen is also performed using the lineal-path function. In Figure 9, when r/D is zero, L_{lwa} values for all specimens are larger than 0.7, which shows that all of the samples include more than 70% of LWAs as planned. L_{lwa} of LW 30 is relatively smaller than that of other samples because the proportion of fine aggregates in LW 30 is larger than that of other cases, whereas it contains less coarse aggregates. On the contrary, L_{lwa} of LW 25 is the largest among the samples, which means that the sample contains a larger proportion of coarse aggregates than other samples. Although the differences of L_{lwa} in Figure 9 are not large enough to show significant differences of the samples, the results obtained from the probability function can be utilized to evaluate the relative aggregate sizes between the LWC specimens.

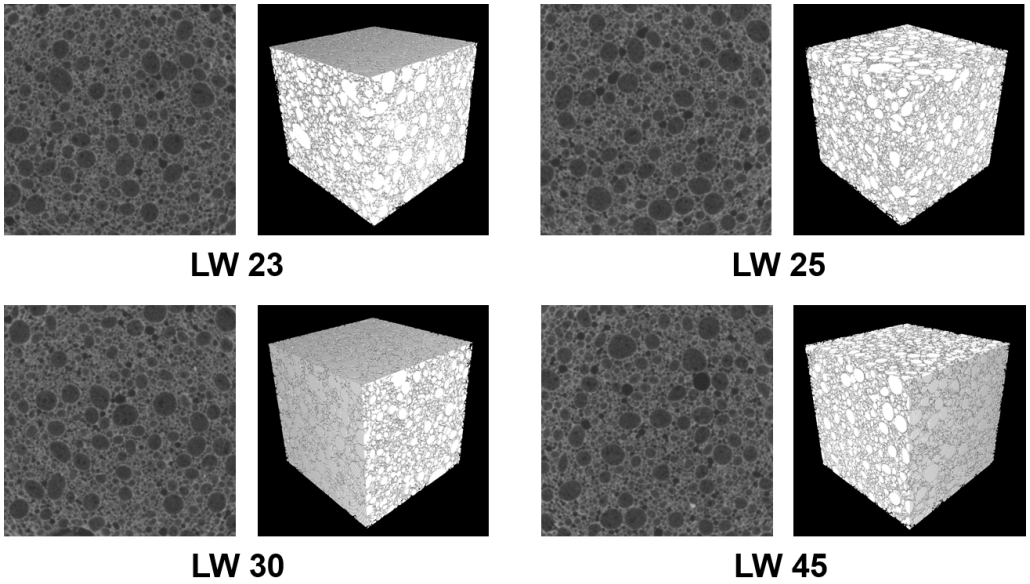

Figure 8. Sample CT images and 3D LWA images of each sample (note: the left figure is the original X-ray CT image, and the right figure is the 3D image.).

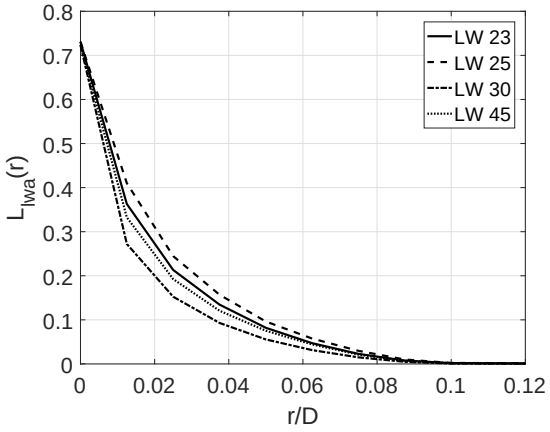

Figure 9. L_{lwa} for the LWC samples (note: the results of r/D range between 0 and 0.12 are only presented here.).

5. Conclusions

In this study, a series of ultra-lightweight concrete specimens less than 500 kg/m^3 densities are designed and produced, and their properties and characteristics are evaluated. An expanded glass, Liaver®, is used as the lightweight aggregate, and different gradings for the lightweight aggregates are adopted to maximize the aggregate contents in the specimens. The effects of gradings on the concrete characteristics and properties are investigated. For the purpose, the virtual specimens that contain more than 70% of aggregates are modeled. The qualities and the characteristics of the specimens are examined using X-ray CT and the lineal-path function, which is a probabilistic description method.

The material properties, such as elastic modulus, compressive strength, and thermal conductivity, are measured using experimental and numerical approaches. The conclusions of this study can be summarized as follows:

- The obtained results show the effect of gradings and the packing algorithm on the material properties of lightweight aggregate concrete.
- All the specimens produced in this study show a higher performance than conventional lightweight concrete based on efficiency factors, while the specimen densities are lower than those of conventional concretes.
- When the volume content of the lightweight aggregates is the same, the lightweight concrete specimen with a larger proportion of finer aggregates shows a larger elastic modulus and compressive strength, while the thermal conductivity of the specimen is larger.
- Lightweight concrete with lower thermal conductivity, while minimizing the loss of mechanical properties, can be produced by using an appropriate grading, although the density of the specimen strongly affects the material properties and becomes larger when the proportion of finer aggregates increases.
- The X-ray CT imaging and the lineal-path function shows potential for examining the relative aggregate size in the concrete specimen.

With the confirmation of the effect of the grading on the material properties, a more in-depth parametric study of different gradings as well as a packing algorithm would be required for further development of ultra-lightweight concrete with higher performance.

Acknowledgments: The project is supported by the German Federal Ministry of Education and Research (BMBF, Project number: 13XP5010B) and the German Academic Exchange Service (DAAD, Ref. no.: 91563255). This work is also supported by the Basic Science Research Program through the National Research Foundation of Korea (NRF) funded by the Ministry of Education (2016R1A6A3A03007804). In addition, the authors want to thank Paul H. Kamm (Helmholtz Centre Berlin) for his assistance in X-ray CT imaging.

Author Contributions: Sang-Yeop Chung conceived and designed the experiments; and Mohamed Abd Elrahman performed the experiments; Sang-Yeop Chung and Dietmar Stephan analyzed the data; Mohamed Abd Elrahman contributed reagents/materials/analysis tools; and Sang-Yeop Chung, Dietmar Stephan and Mohamed Abd Elrahman wrote the paper.

Conflicts of Interest: The authors declare no conflict of interest.

References

1. Narayanan, N.; Ramamurthy, K. Structure and properties of aerated concrete: A review. *Cem. Concr. Compos.* **2000**, *22*, 321–329.
2. Mindess, S.; Young, J.F.; Darwin, D. *Concrete*, 2nd ed.; Prentice Hall: Upper Saddle River, NJ, USA, 2002; pp. 4–48.
3. Neville, A.M. *Properties of Concrete*; Wiley: Hoboken, NJ, USA, 2012; pp. 10–24.
4. Korat, L.; Ducman, V.; Legat, A.; Mirtic, B. Characterisation of the pore-forming process in lightweight aggregate based on silica sludge by means of X-ray micro-tomography (micro-CT) and mercury intrusion porosimetry (MIP). *Cem. Concr. Res.* **2013**, *39*, 6997–7005.
5. Sales, A.; Souza, F.R.; Santos, W.N.; Zimer, A.M.; Almeida, F.C.R. Lightweight composite concrete produced with water treatment sludge and sawdust: Thermal properties and potential application. *Constr. Build. Mater.* **2010**, *24*, 2446–2453.
6. Chabannes, M.; Benezet, J.-C.; Clerc, L.; Garcia-Diaz, E. Use of raw rice husk as natural aggregate in a lightweight insulating concrete: An innovative application. *Constr. Build. Mater.* **2014**, *70*, 428–438.
7. Wu, Y.; Wang, J.-Y.; Monteiro, P.J.M.; Zhang, M.-H. Development of ultra-lightweight cement composites with low thermal conductivity and high specific strength for energy efficient buildings. *Constr. Build. Mater.* **2015**, *87*, 100–112.
8. Colangelo, F.; Messina, F.; Cioffi, R. Recycling of MSWI fly ash by means of cementitious double step cold bonding pelletization: Technological assessment for the production of lightweight artificial aggregates. *J. Hazard. Mater.* **2015**, *299*, 181–191.
9. Lihua, Z.; Yunsheng, Z.; Chuanbei, L.; Laibao, L.; Kaijing, T. Study on microstructure and bond strength of interfacial transition zone between cement paste and high-performance lightweight aggregates prepared from ferrochromium slag. *Constr. Build. Mater.* **2017**, *142*, 31–41.
10. Bogas, J.A.; Cunha, D. Non-structural lightweight concrete with volcanic scoria aggregates for lightweight fill in building's floors. *Constr. Build. Mater.* **2017**, *135*, 151–163.
11. Colangelo, F.; Cioffi, R.; Liguori, B.; Iucolano, F. Recycled polyolefins waste as aggregates for lightweight concrete. *Compos. Part B* **2016**, *106*, 234–241.
12. Guneyisi, E.; Gesoglu, M.; Ali Azez, O.; Oz, H.O. Effect of nano silica on the workability of self-compacting concretes having untreated and surface treated lightweight aggregates. *Constr. Build. Mater.* **2016**, *115*, 371–380.
13. Youm, K.-S.; Moon, J.; Cho, J.-Y.; Kim, J.J. Experimental study on strength and durability of lightweight aggregate concrete containing silica fume. *Constr. Build. Mater.* **2016**, *114*, 517–527.
14. European Union. EuroLightCon LWAC material properties state-of-the-art. In *Economic Design and Construction with Light Weight Aggregate Concrete*; Brite-EuRam III; European Union: Brussels, Belgium, 1998; pp. 4–178.
15. Wang, H.Y.; Tsai, K.C. Engineering properties of lightweight aggregate concrete made from dredged silt. *Cem. Concr. Compos.* **2006**, *28*, 481–485.
16. Schackow, A.; Effting, C.; Folgueras, M.V.; Guths, S.; Mendes, G.A. Mechanical and thermal properties of lightweight concretes with vermiculite and EPS using air-entraining agent. *Constr. Build. Mater.* **2014**, *57*, 190–197.
17. Yu, R.; van Onna, D.V.; Spiesz, P.; Yu, Q.L.; Brouwers, H.J.H. Development of ultra-lightweight fibre reinforced concrete applying expanded waste glass. *Constr. Build. Mater.* **2016**, *112*, 690–701.

18. Mehta, P.K.; Monteiro, P.J.M. *Concrete: Microstructure, Properties and Materials*, 3rd ed.; McGraw-Hill: New York, NY, USA, 2005; pp. 13–37.
19. Liu, X.; Chia, K.S.; Zhang, M.-H. Development of lightweight concrete with high resistance to water and chloride-ion penetration. *Cem. Concr. Compos.* **2010**, *32*, 757–766.
20. Andreasen, A.H.M.; Andersen, J. Über die Beziehungen zwischen Kornabstufungen und Zwischenraum in Produkten aus losen Körnern. *Kolloid Z.* **1930**, *50*, 217–228. (In German)
21. Funk, J.E.; Dinger, D.R. *Predictive Process Control of Crowded Particulate Suspensions: Applied to Ceramic Manufacturing*; Kluwer Academic Publishers: Dordrecht, The Netherlands, 1994; pp. 123–129.
22. Brouwers, H.J.H.; Radix, H.J. Self compacting concrete: Theoretical and experimental study. *Cem. Concr. Res.* **2005**, *35*, 2116–2136.
23. Huesken, G.; Brouwers, H.J.H. A new mix design concept for earth-moist concrete: A theoretical and experimental study. *Cem. Concr. Res.* **2008**, *35*, 1246–1259.
24. Shi, Y.; Zhang, Y. Simulation of random packing of spherical particles with different size distributions. *Appl. Phys. A Mater.* **2008**, *92*, 612–626.
25. Kwan, A.K.H.; Fung, W.W.S. Packing density measurement and modelling of fine aggregate and mortar. *Cem. Concr. Compos.* **2009**, *31*, 349–357.
26. Sobolev, K.; Amirjanov, A. Application of genetic algorithm for modeling of dense packing of concrete aggregates. *Constr. Build. Mater.* **2010**, *24*, 1449–1455.
27. Abd Elrahman, M.; Hillemeier, B. Combined effect of fine fly ash and packing density on the properties of high performance concrete: An experimental approach. *Constr. Build. Mater.* **2014**, *58*, 225–233.
28. Fennis, S.A.A.M.; Walraven, J.C.; den Uijl, J.A. The use of particle packing models to design ecological concrete. *Heron* **2009**, *54*, 185–204.
29. Hunger, M. *An Integral Design Concept for Ecological Self-Compacting Concrete*; CIP-Data Library Technische Universiteit Eindhoven: Eindhoven, The Netherlands, 2010; pp. 58–69.
30. Brouwers, H.J.H. Particle-size distribution and packing fraction of geometric random packings. *Phys. Rev. E* **2006**, *74*, 031309.
31. Huesken, G.; Brouwers, H.J.H. On the early-age behavior of zero-slump concrete. *Cem. Concr. Res.* **2012**, *42*, 501–510.
32. Yu, Q.L.; Spiesz, P.; Brouwers, H.J.H. Ultra-lightweight concrete: Conceptual design and performance evaluation. *Cem. Concr. Compos.* **2015**, *61*, 18–28.
33. International Organization for Standardization. *Plastics—Determination of Thermal Conductivity and Thermal Diffusivity—Part 2: Transient Plane Heat Source (Hot Disk) Method*; 22007-2:2015; DIN EN 1990; ISO: Geneva, Switzerland, 2015.
34. European Committee for Standardization. *Testing Hardened Concrete—Part 4: Compressive Strength—Specification for Testing Machines*; EN 12390-4:2000; CEN: Brussels, Belgium, 2000.
35. Jia, T.; Zhang, Y.; Chen, J.K. Simulation of granular packing of particles with different size distributions. *Comput. Mater. Sci.* **2012**, *51*, 172–180.
36. Sobolev, K.; Amirjanov, A. The development of a simulation model of the dense packing of large particulate assemblies. *Powder Technol.* **2004**, *141*, 155–160.
37. *Abaqus*, version v2016; Dassault Systemes: Velizy-Villacoublay Cedex, France, 2016.
38. Ramamurthy, K.; Nambiar, E.K.K.; Ranjani, G.I.S. A classification of studies on properties of foam concrete. *Cem. Concr. Compos.* **2009**, *31*, 388–396.
39. Jankowiak, T.; Lodygowski, T. Identification of parameters of concrete damage plasticity constitutive model. *Found. Civ. Environ. Eng.* **2005**, *6*, 53–69.
40. Incropera, F.P.; Dewitt, D.P.; Bergman, T.L.; Lavine, A.S. *Fundamentals of Heat and Mass Transfer*; John Wiley and Sons: Hoboken, NJ, USA, 2006; pp. 127–145.
41. Jeffers, A.E.; Beat, P.A. Generalized shell heat transfer element for modeling the thermal response of non-uniformly heated structures. *Finite Elem. Anal. Des.* **2014**, *83*, 58–67.
42. Kmiecik, P.; Kaminski, M. Modelling of reinforced concrete structures and composite structures with concrete strength degradation taken into consideration. *Arch. Civ. Mech. Eng.* **2011**, *11*, 623–636.
43. Lu, B.; Torquato, S. Lineal-path function for random heterogeneous materials. *Phys. Rev. A* **1992**, *45*, 922–929.
44. Torquato, S. *Random Heterogeneous Materials*; Springer Nature: New York, NY, USA, 2002; pp. 327–335.

45. Chung, S.-Y.; Abd Elrahman, M.; Stephan, D.; Kamm, P.H. Investigation of characteristics and responses of insulating cement paste specimens with Aer solids using X-ray micro-computed tomography. *Constr. Build. Mater.* **2016**, *118*, 204–215.
46. Moreno, F.G.; Fromme, M.; Banhart, J. Real-time X-ray radioscopy on metallic foams using a compact micro-focus source. *Adv. Eng. Mater.* **2004**, *6*, 416–420.
47. Otsu, N. A threshold selection method from gray-level histograms. *Man. Cybern.* **1979**, *9*, 62–66.
48. Cui, F.; Wang, X.L.; Peng, S.; Vogel, C. A Parallel Algorithm for Quasi Euclidean Distance Transform. *J. Image Graph.* **2004**, *6*, 1–6.
49. Hueckler, A. *Trag-Und Verformungsverhalten von Biegebeanspruchten Bauteilen aus Infraleichtbeton (ILC)*; Sierke Verlag: Göttingen, Germany, 2016; pp. 112–114. (In Germany)